

Impact of Static Liquid Height on Hydrodynamics of the Thermolysis Reactor in the Cu-Cl Cycle for Hydrogen Production

M. W. Abdulrahman¹, N. Nassar²

¹Rochester Institute of Technology (RIT)
Dubai, UAE
mwacad@rit.edu; nin8507@g.rit.edu
²Rochester Institute of Technology (RIT)
Dubai, UAE

Abstract - This study specifically examines the effect of static liquid height in the hydrodynamics of the thermolysis reactor in the copper chlorine cycle for hydrogen production. The paper used a 3D computational fluid dynamics (CFD) model to examine the gas holdup behaviour at various static liquid heights, ranging from 45 to 65 m. The model, confirmed using experimental data and compared to a two-dimensional counterpart, accurately depicts the trend of gas holdup. It has a maximum error of 48.6%, indicating that gas holdup decreases as static liquid height rise. The three-dimensional model provides crucial insights into the reactor's performance and improves strategies for hydrogen production.

Keywords: static liquid height; 3D CFD; gas holdup; hydrogen production; Cu-Cl cycle

1. Introduction

Hydrogen is essential to sustainable energy solutions because it drives the shift toward greener energy systems. Its ability to reduce greenhouse gas emissions makes it vital to climate change mitigation. Hydrogen production via thermochemical cycles is innovative. These cycles can break down water with using nuclear reactors via multiple chemical processes. The copper-chlorine (CuCl) cycle, discovered at Argonne National Laboratories (ANL), is efficient even at low temperatures [1,2]. The CuCl cycle uses oxygen to generate heat and operates at high temperatures. Scientists have tried many methods to efficiently convey heat in the oxygen reactor. Studies show that direct contact heat transfer (DCHT), which involves returning 600°C oxygen gas into the reactor, successfully heats molten CuCl [3,4]. This method improves reactor efficiency and uses oxygen gas as a thermal medium. Slurry bubble column reactors (SBCRs) help the CuCl cycle produce oxygen. These multiphase reactors simplify gas-liquid-solid interactions. The reactor bed bubbles with sparger-injected gas. SBCR temperature may be precisely controlled due to liquid specific heat. This makes them versatile commercially. Scaling SBCRs involves knowledge of kinetics, hydrodynamics, heat and mass transport, and other aspects. The gas holdup, which represents the reactor's gas volume fraction, is an important SBCR performance measure. SBCR design and operation in industry require careful management of these factors. The literature consolidates study results, highlighting novel methodologies, experimental investigations, and CFD analyses that affect reactor design and operation.

Abdulrahman [3-12] studied material and thermal balances in these systems' scale-up. His research has modified continuous stirred tank reactors (CSTRs) using half-pipe jackets, spiral baffled jackets, and helical internal tubes to maximize heat transfer and reduce thermal resistance. Abdulrahman's research focused on using nuclear reactors as heat sources, notably the CANDU Super Critical Water Reactor (SCWR) and the High Temperature Gas Reactor. His findings suggested that the CANDU-SCWR needed higher heat transfer rates to improve process efficiency. To optimize thermolysis, Abdulrahman proposed heating and re-injecting oxygen gas directly into the reactor in 2018 [4]. Abdulrahman [5] investigated thermolysis-compatible chemical reactors for oxygen production. He believes the bubble column reactor is best. Using molten CuCl and O₂ gas in thermolysis reactor thermal hydraulics experiments provides numerous obstacles. To emulate thermal hydraulic behaviours of the original substances, Abdulrahman [13-14] discovered substitute materials by dimensional analysis. These convenient, affordable replacements make experimentation safer and cooler. Abdulrahman investigated SBCR thermal hydraulics experimentally [4,15-16]. The study examined how superficial gas velocity (U_{gs}) and static liquid height (H) affect the bubble column reactor's gas holdup (α_g), volumetric heat transfer coefficient (U_v), and liquid temperature. These effects were formulated as empirical equations. Experiments show that increasing U_{gs} leads

to higher U_v , liquid temperature, and α_g . Abdulrahman [17] measured SBCR transition velocity experimentally. Increasing H decreases the transition velocity between homogeneous and churn turbulent flow regimes, according to experiments. No slug flow regime was detected in industrial SBCRs. Abdulrahman and Nassar [18] reviewed Eulerian CFD for BCR and SBCR analysis. They evaluated research that changed reactor design, superficial gas velocity, pressure, and solid concentration to determine their effects on thermal hydraulics. The review found that the Eulerian CFD model accurately predicts BCR and SBCR performance.

Matiazzo et al. [19] examined drag coefficients, coalescence, and breakdown models in the churn turbulent flow regime using 3D CFD. The study included 12 coalescence and breakdown configurations. The findings stressed the importance of adopting the correct breakage and coalescence models, as the breakdown model considerably affected flow predicts more than the coalescence model. Compared to experimental findings, the Schiller and Naumann [20] model predicted drag closure best. The CFD simulations matched the experimental results with low gas velocity and gas holdup errors. Predictions of gas velocity in the reactor centre were more accurate than those at the walls, when simulations overestimated experimental measurements. Ertekin et al. [21] adjusted column radius and superficial gas velocity to verify Fletcher et al. (2017) CFD simulations. Fletcher et al. [22] validated two-phase Euler-Euler models with a pre-set single bubble size. The liquid phase was analysed using a typical k- ϵ turbulence approach. Ertekin et al. verified Fletcher's models, finding only a small percentage difference in holdup studies.

Yan et al. [23] examined BCR hydrodynamics using several drag models. The reactor was 30 cm wide and 660 cm tall, with a gas sparger 20 cm from the base and 128 holes of 5mm diameter. The study compared two- and three-dimensional CFD models to electrical resistance tomography data. Radial gas holdup increased with superficial gas velocity in the cold-water air model of the bubble column. Increased internal pressure increased radial gas holdup, especially near the column centre. These trends matched experimental results and two and three CFD models. Adam and Tuwaechi [24] investigated gas holdup using a two-phase CFD model with coarse and fine meshes using Eulerian-Eulerian approach and k- ϵ turbulence model. Their simulated BCR was 96 cm tall and 19 cm wide. The model revealed that increasing the time step increased the volume fraction, with 0.005 mesh resolutions yielding crisper observations. They also found that gas pressure peaked near the inlet and declined as it moved away.

Pourtousi et al. [25] studied bubble column regimes using Euler-Euler simulation. The SBC in their three-dimensional CFD model was 260 cm tall and 28.8 cm wide. Simulated and experimental data were compared to assess accuracy. A 3 mm bubble diameter predicted superficial gas velocities from 0.0025 to 0.015 m/s in the bulk region. In a homogeneous domain, a single bubble diameter can be computationally efficient and effective, but in a heterogeneous regime, a diversity of bubble sizes plus a proper drag model may increase accuracy. Homogeneous flows have homogeneous bubble sizes and shapes with negligible interaction, but heterogeneous flows have bubbles ranging from 0.05 mm to 50 mm, impacting reactor dynamics. Abdulrahman used 2D CFD simulations to study SBCR hydrodynamics and DCHT [26-30]. The study investigated how liquid height, superficial gas velocity, and solid concentration affect SBCR gas holdup, volumetric heat transfer coefficient, and temperature distributions. Abdulrahman and Nassar [31-33] used 3D CFD to study oxygen reactor hydrodynamics.

This research intends to investigate the hydrodynamics of the oxygen reactor in the Cu-Cl cycle, considering the pressing need to tackle climate change and the potential of hydrogen as a sustainable energy carrier. The study employs three-dimensional computational fluid dynamics (CFD) models utilizing the ANSYS Fluent software. Validation is accomplished by comparing the simulation findings with empirical data obtained from previous experimental study, therefore guaranteeing the accuracy and dependability of the results.

2. CFD Analysis

This work uses computational fluid dynamics (CFD) simulations to analyse a three-dimensional system. The simulations include a Eulerian-Eulerian model and a Eulerian sub-model, in conjunction with a pressure-based solver. The mathematical equations utilized in the computational fluid dynamics (CFD) investigation are outlined in Table 1. These equations are specifically designed for the gas phase. Due to their similarity to the equations for the gas phase, the equations for the slurry phase are not restated in order to be concise.

Table 1: Details of equations used in the 3D CFD simulations.

Description [reference]	Equation
Volume equation [34]	$V_g = \int_V \alpha_g dV$
Continuity equation in 3D Polar coordinates (r, θ, y) [3]	$\nabla \cdot V_g = \frac{\partial v_{r,g}}{\partial r} + \frac{v_{r,g}}{r} + \frac{1}{r} \frac{\partial v_{\theta,g}}{\partial \theta} + \frac{\partial v_{y,g}}{\partial y} = 0$
Momentum equation in 3D Polar coordinates [3]	$\rho_g \alpha_g \left(\frac{\partial v_r}{\partial t} + v_r \frac{\partial v_r}{\partial r} + \frac{v_\theta}{r} \frac{\partial v_r}{\partial \theta} + v_y \frac{\partial v_r}{\partial y} - \frac{v_\theta^2}{r} \right) = -\alpha_g \frac{\partial P}{\partial r} + \alpha_g \mu_{g,eff} \left[\frac{1}{r} \frac{\partial}{\partial r} \left(r \frac{\partial v_r}{\partial r} \right) + \frac{1}{r^2} \frac{\partial}{\partial \theta} \left(r^2 \frac{\partial v_\theta}{\partial \theta} \right) + \frac{\partial^2 v_r}{\partial y^2} \right]$
	$\rho_g \alpha_g \left(\frac{\partial v_\theta}{\partial t} + v_r \frac{\partial v_\theta}{\partial r} + \frac{v_\theta}{r} \frac{\partial v_\theta}{\partial \theta} + v_y \frac{\partial v_\theta}{\partial y} + \frac{v_r v_\theta}{r} \right) = -\alpha_g \frac{1}{r} \frac{\partial P}{\partial \theta} + \alpha_g \mu_{g,eff} \left[\frac{1}{r} \frac{\partial}{\partial r} \left(r \frac{\partial v_\theta}{\partial r} \right) + \frac{1}{r^2} \frac{\partial}{\partial \theta} \left(r^2 \frac{\partial v_\theta}{\partial \theta} \right) + \frac{\partial^2 v_\theta}{\partial y^2} \right]$
	$\rho_g \alpha_g \left(\frac{\partial v_y}{\partial t} + v_r \frac{\partial v_y}{\partial r} + \frac{v_\theta}{r} \frac{\partial v_y}{\partial \theta} + v_y \frac{\partial v_y}{\partial y} \right) = -\alpha_g \frac{\partial P}{\partial y} + \alpha_g \mu_{g,eff} \left[\frac{1}{r} \frac{\partial}{\partial r} \left(r \frac{\partial v_y}{\partial r} \right) + \frac{1}{r^2} \frac{\partial}{\partial \theta} \left(r^2 \frac{\partial v_y}{\partial \theta} \right) + \frac{\partial^2 v_y}{\partial y^2} \right]$
Energy equation in 3D Polar coordinates [3]	$\alpha_g \rho_g C \left(\frac{\partial T_g}{\partial t} + v_{r,g} \frac{\partial T_g}{\partial r} + \frac{v_{\theta,g}}{r} \frac{\partial T_g}{\partial \theta} + v_{y,g} \frac{\partial T_g}{\partial y} \right) = \tau_g : \nabla V_g + k_g (\nabla^2 T_g)$
Effective density	$\hat{\rho}_g = \alpha_g \rho_g$
Drag force [34]	$M_D = \frac{\rho_g f}{6 \tau_b} d_b A_i (V_g - V_l)$
Interfacial area [34]	$A_i = \frac{6 \alpha_g (1 - \alpha_g)}{d_b}$
Schiller-Naumann drag equation [20]	$C_D = \begin{cases} \frac{24 (1 + 0.15 \Re_b^{0.687})}{\Re_b} & \Re_b \leq 1000 \\ 0.44 \Re_b & \Re_b > 1000 \end{cases}$

The dimensions of the reactor in this study are established according to the Helium-Water bubble column reactor investigated by Abdulrahman [15-17]. However, the material properties have been modified to correspond to oxygen and Cupreous Chloride. Abdulrahman's property comparison [24-25] indicates that the O₂-CuCl system and the Helium-Water (He-H₂O) systems exhibit similarities. In order to achieve consistency, the superficial gas velocity of the O₂-CuCl system is adjusted precisely to match the Reynolds number of the He-H₂O system. The reactor utilized in this investigation possesses a cylindrical configuration, measuring 21.6 cm in diameter and 91.5 cm in height. The gas is injected into the bubble

column reactor using a gas distributor of the sparger type, which has six arms. Each arm is equipped with 12 orifices, each having a diameter of 0.3 cm, resulting in a total of 72 holes.

The turbulence model used in this study is the Reynolds-Averaged Navier-Stokes (RANS) models, namely the $k-\epsilon$ and $k-\omega$ models. These models are known for being the most cost-effective methods to estimate complex turbulent flows. These models have the ability to simulate a wide range of turbulent flows and heat transfer processes with a satisfactory level of accuracy. The RNG $k-\epsilon$ model is selected for its superior accuracy and reliability across a wider range of flows in comparison to the traditional $k-\epsilon$ model. This model is specifically appropriate for simulating turbulent flow associated with churn, which is the main emphasis of this work. The $k-\epsilon$ sub-model employed is the dispersed turbulence model, chosen for its ability to accurately account for the distinct phase densities of liquid and gas, as well as the low concentrations of the gas phase. Moreover, this turbulence model is more cost-effective in terms of computational resources compared to the per-phase turbulence model. The wall boundary conditions are typically modelled using the standard wall function, which is widely employed in industries due to its ability to yield satisfactory results for a range of flows that are bounded by walls.

The ANSYS Fluent software, is employed to model the 3D Bubble Column Reactor (BCR) in this study. The setup and boundary conditions for the simulation are determined using ANSYS Fluent. The Bubble Column Reactor (BCR) utilizes a hexahedron mesh, and mesh independence is performed to determine the optimal mesh size that balances computational costs with satisfactory outcomes. The ultimate mesh consists of 26,825 nodes and 24,396 elements, resulting in a 3% disparity in the gas holdup when employing more refined meshes (Fig. 1). The simulated BCR is characterized by three boundaries: the inlet, outflow, and wall conditions. The inlet boundary condition is established by specifying a superficial gas velocity and assuming a gas holdup of 1. The outlet pressure is adjusted to match the ambient pressure, and the walls of the reactor are assumed to have no-slip conditions for both phases. The turbulent kinetic energy and dissipation rate at the inlet and outflow are determined over 5,000 iterations, as accurately estimating these for turbulent models is difficult.

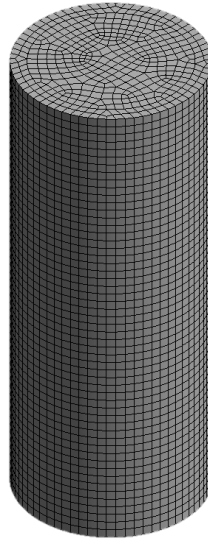


Fig. 1 BCR hexahedron mesh.

1.1 3. Results

3.1. Gas holdup versus static liquid height (H)

Figure. 2 shows the three-dimensional curves of the gas holdup versus the static liquid height (H) and the superficial gas velocity (U_{gs}). Figure 3 depicts the effects of varying H (45, 55, 65cm) on the gas holdup while varying U_{gs} for an O_2 -CuCl system. Figures 4-6 show the contours of the cut sections of the BCR taken

in the centre of the XY, and ZY planes. Additional cut sections are taken at various heights on the ZX plane within the reactor at heights 10, 20 and 30 cm from the base of the reactor to allow for a more detailed contour of α_g . It is clear from the contours that the gas holdup is not symmetrical on the XY, ZY and the ZX planes demonstrating that the behaviour of the gas holdup is strongly three dimensional. It is observed that as the H increases the α_g decreases. At a superficial gas velocity of 0.085 m/s it is observed that the gas holdup decreases by 20% when increasing H from 45 cm to 65 cm.

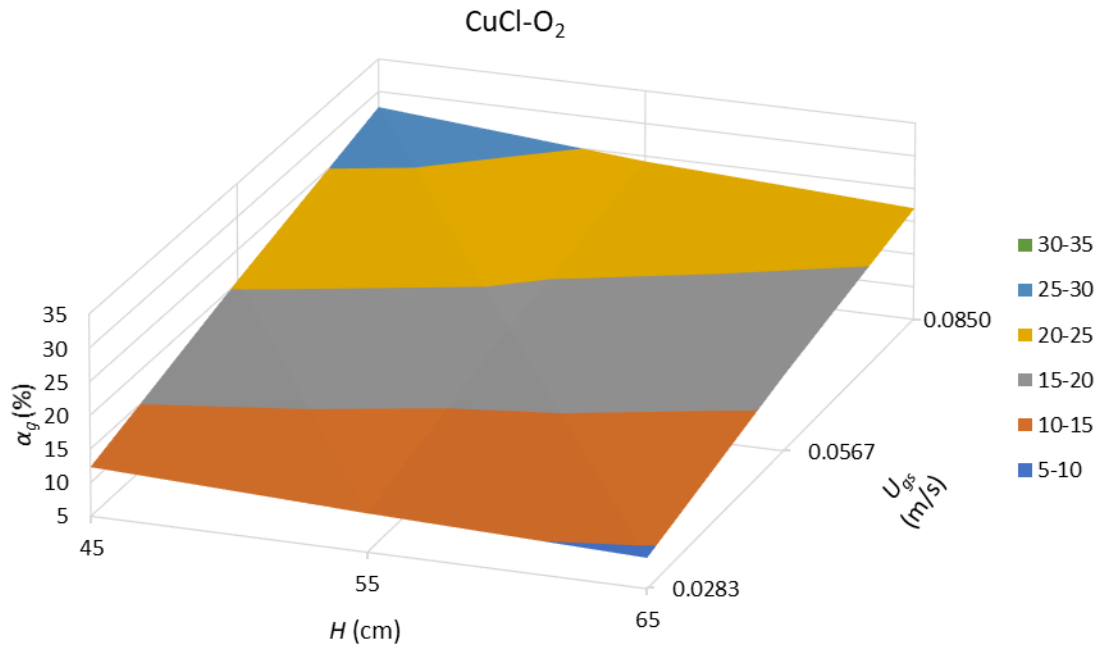


Fig. 2 Average gas holdup versus static liquid height and superficial gas velocity of CuCl-O₂.

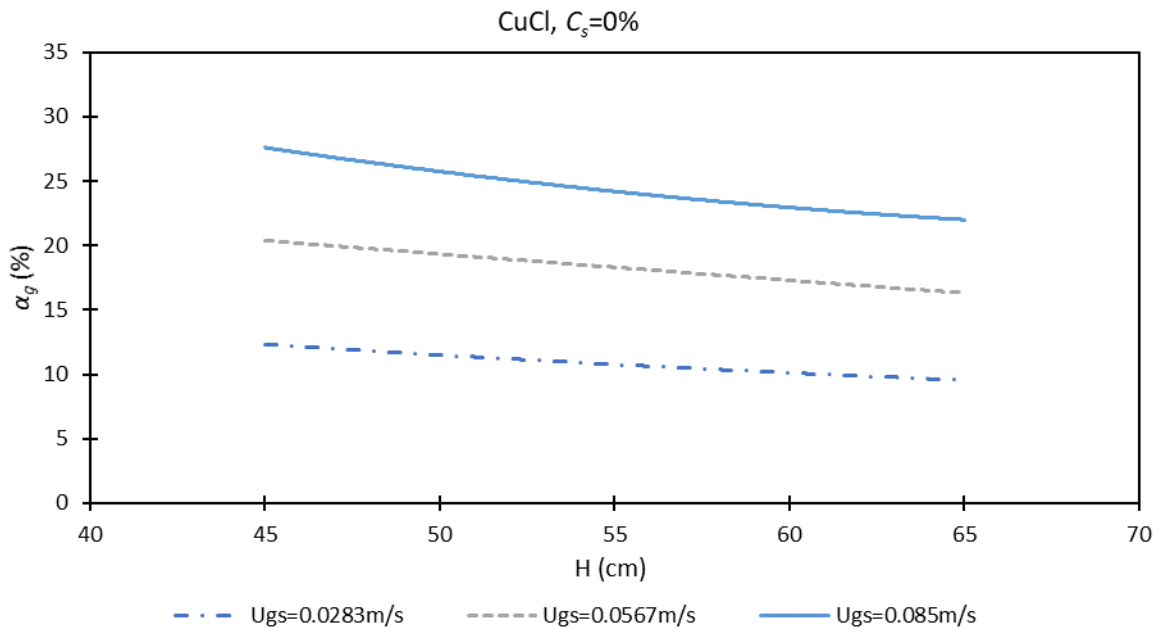


Fig. 3 Average gas holdup versus static liquid height of CuCl-O₂ at different superficial gas velocities.

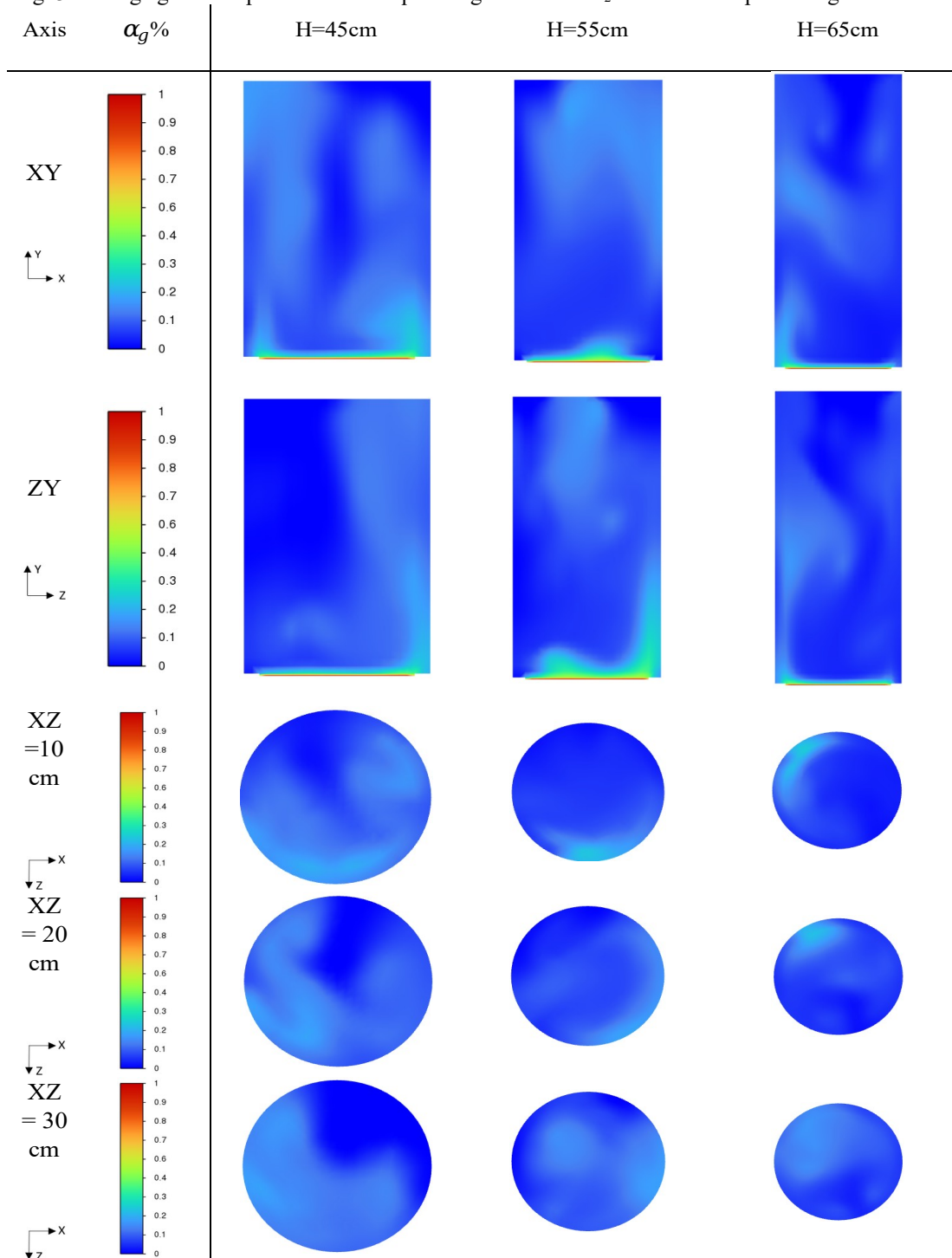


Fig. 4 Oxygen-Cupreous Chloride gas holdup contours for $U_{gs}=0.0283$ m/s.

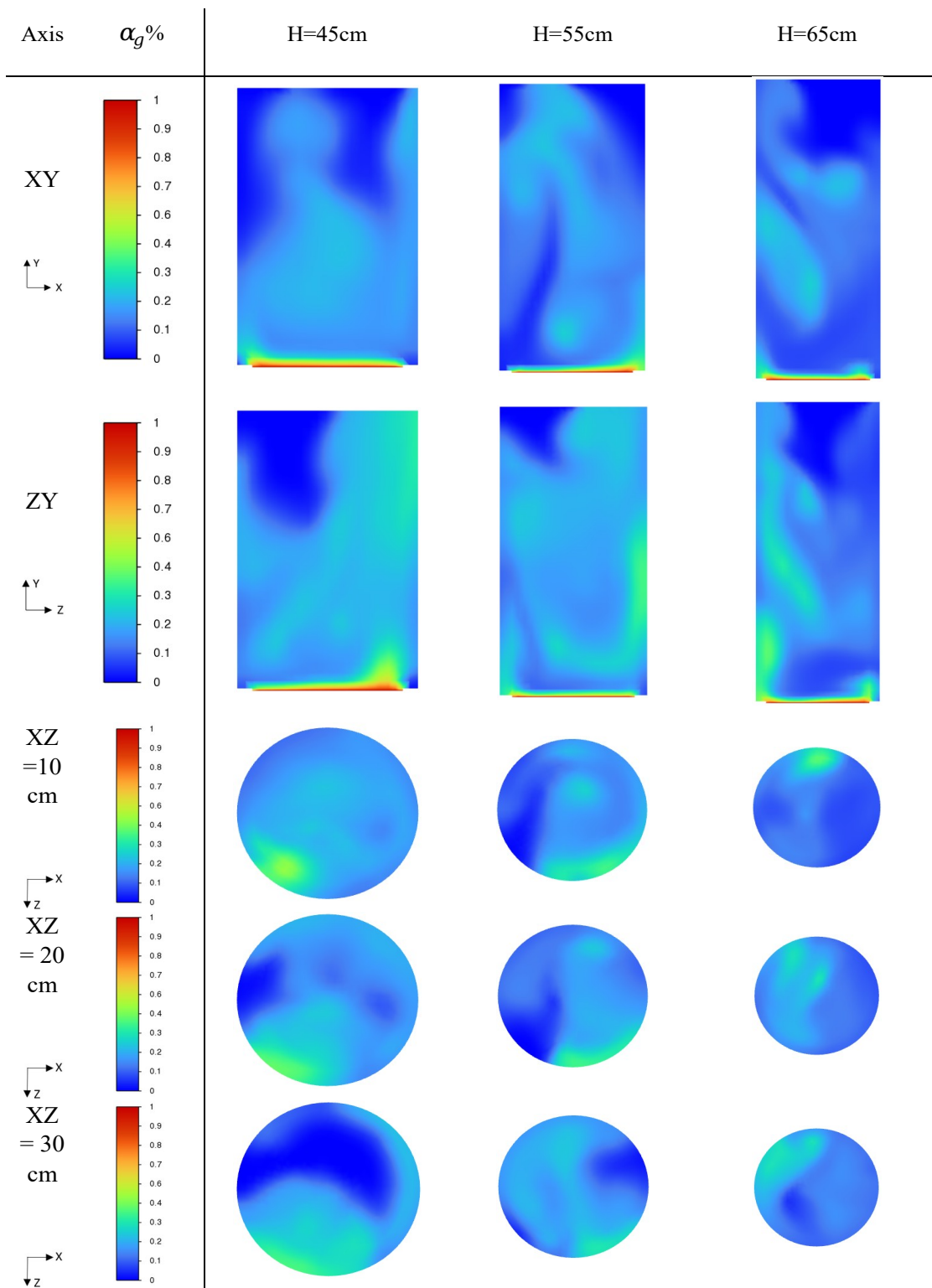


Fig. 5 Oxygen-Cupreous Chloride gas holdup contours for $U_{gs}=0.0567$ m/s.

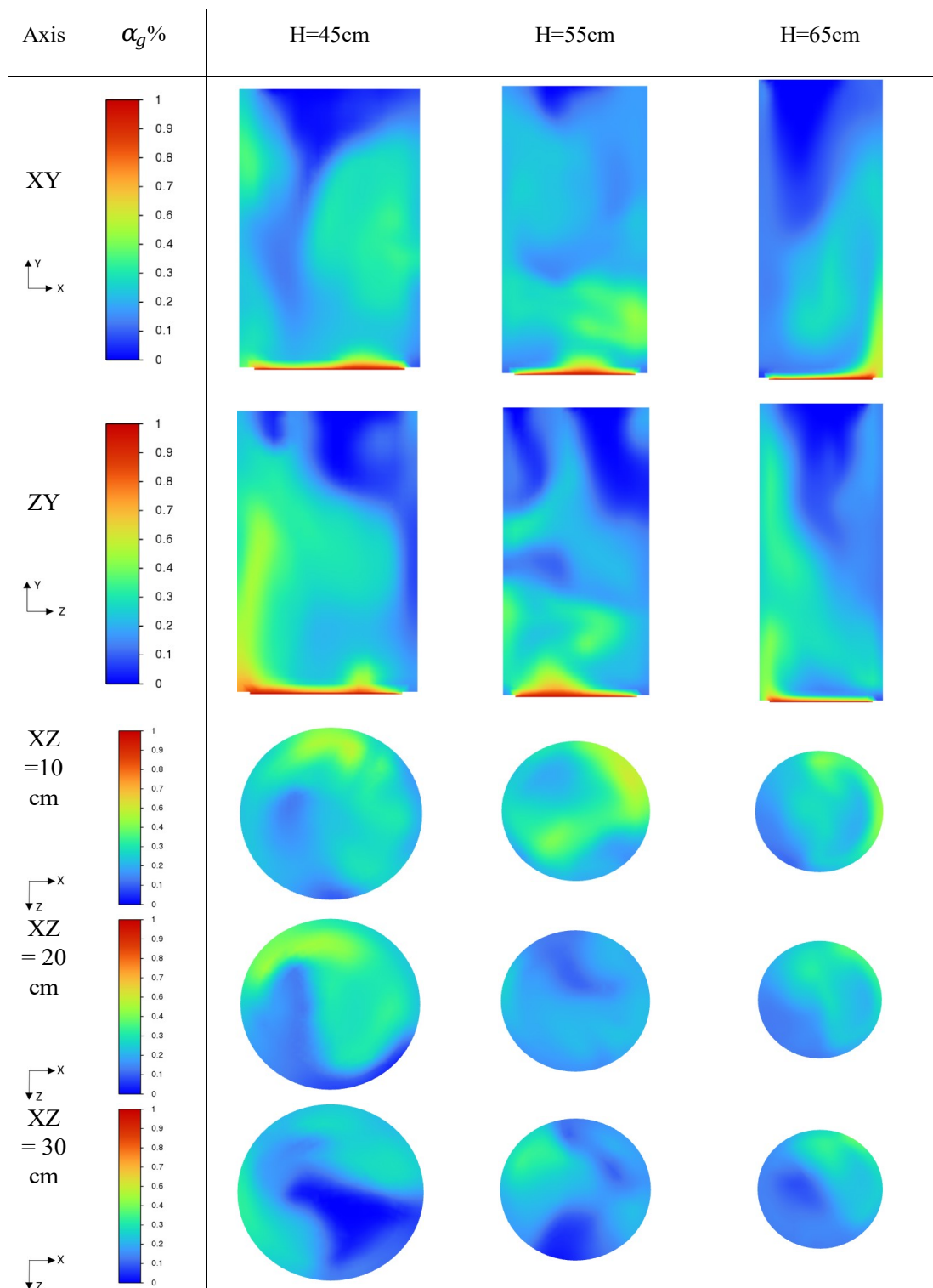


Fig. 6 Oxygen-Cupreous Chloride gas holdup contours for $U_{gs}=0.085$ m/s.

3.2. Comparative Analysis of 3D CFD Models: Water-Helium vs. Copper Chloride-Oxygen Systems

Table 2 presents a comparison of the hydrodynamics dimensionless groups between the actual materials (CuCl and O₂) and the simulated materials (He and H₂O), as described in Abdulrahman's study [13-14]. The density ratio of gas to liquid is the primary source of error in the dimensionless groups, with a magnitude of 11.311%. Table 3 displays the calculated gas holdup values for both the actual and simulated materials, along with the corresponding percentage of errors resulting from their disparity. The data clearly indicates that the maximum percentage inaccuracy is 48.6%. Furthermore, it is evident that the gas holdup values in the actual materials are typically underestimated compared to those in the simulated materials. The superficial gas velocities of the actual substances were modified to produce similar effects as those in the simulated substances. The elevated percentage error can be attributed to the cumulative effect of the percentage errors generated by each of the hydrodynamic dimensionless parameters, as indicated in Table 2. Additionally, the intricate nature of the three-dimensional multiphase system also contributes to this error. The 3D CuCl-O₂ simulation well replicated the patterns and behaviours observed in the SBCR.

Table 2 Percent error analysis of dimensionless groups in actual vs. experimental materials [13-14].

Dimensionless Group	Actual Material	Experimental Materials	Error%
$\frac{\rho_g}{\rho_l}$	0.000121	0.000135	11.311
$\frac{\mu_g}{\mu_l}$	0.021756	0.023	6.908
$\frac{\Re_l^2}{We_l}$	76473868 (D_R =1m)	76085070 (D_R =1m)	0.508

Table 3 Percent Error Analysis for Evaluating Superficial Gas Velocity and Gas Holdup in Water-Helium vs. Cuprous Chloride-Oxygen Systems.

Water-Helium		Cuprous Chloride-Oxygen		Percent Error (%)
U_{gs} (m/s)	α_g (%)	U_{gs} (m/s)	α_g (%)	
H=45 cm				
0.05	16.0	0.0283	12.3	29.9
0.1	24.4	0.0576	20.4	19.6
0.15	31.3	0.085	27.6	13.3
H=55 cm				
0.05	15.0	0.0283	10.8	39.4
0.1	22.7	0.0576	18.3	24.0
0.15	28.0	0.085	24.2	15.7
H=65 cm				
0.05	14.2	0.0283	9.5	48.6
0.1	21.7	HTF-575-9	16.3	33.1
0.15	26.5	0.085	22.0	20.5

In it can be noticed the behaviour of the gas holdup the static

Fig. 4, that of the with liquid

height is similar in both systems of H₂-H₂O and O₂-CuCl, where the gas holdup decreases with increasing the static liquid height.

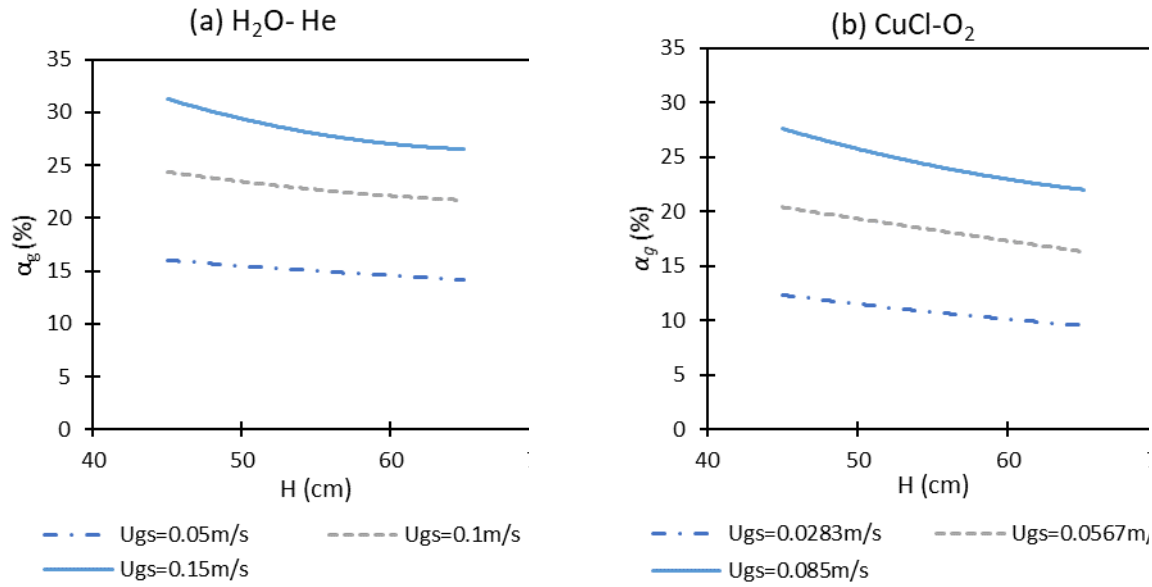


Fig. 4 Comparison of Average Gas Holdup Versus Static Liquid Height for (a) Water-Helium system $C_s=0\%$ (b) Cupreous Chloride-Oxygen system.

4. Conclusions

The objective of this study is to confirm the suitability of substitute materials, especially helium gas and liquid water, as replacements for the actual materials, namely oxygen gas and molten CuCl, in the oxygen bubble column reactor used for the thermochemical copper-chlorine (Cu-Cl) cycle of hydrogen production. The validation process involves conducting 3D computational fluid dynamics (CFD) simulations using ANSYS Fluent software. The simulations specifically focus on the CuCl-O₂ system and examine different static liquid heights. The analysis confirms that the gas holdup patterns remain consistent across both three-dimensional computational fluid dynamics (CFD) models. In addition, the gas holdup in the 3D CFD results of the O₂-CuCl system is consistently lower than that in the 3D CFD findings of the He-H₂O system.

List of Symbols

A_i	Interfacial area concentration	v	Velocity field
C	Specific heat	V_g	Volumes of gas
C_D	Drag coefficient	V_l	Volumes of liquid
d_b	Bubble diameter	U_{gs}	Superficial gas velocity
g	Gravitational acceleration	α_g	Gas holdup
H	Height	μ_{eff}	Effective viscosity
M_i	Total interfacial forces between the phases	μ_g	Dynamic viscosity gas
P	Phase pressure	μ_l	Dynamic viscosity liquid
$Q_{g,l}$	Intensity of heat exchange between the gas and liquid phases	ρ_g	Density, gas
Re	Reynolds number	ρ_l	Density, liquid
T	Temperature	$\bar{\tau} : \nabla v$	Viscous stress tensor contracted with the velocity gradient

References

- [1] Lewis, M. A., M. Serban, and J. K. Basco. "Generating hydrogen using a low temperature thermochemical cycle." In *Proceedings of the ANS/ENS 2003 Global International Conference on Nuclear Technology, New Orleans*. 2003.
- [2] Serban, M., M. A. Lewis, and J. K. Basco. "Kinetic study of the hydrogen and oxygen production reactions in the copper-chloride thermochemical cycle." *AIChE 2004 spring national meeting, New Orleans, LA*. 2004.
- [3] Abdulrahman, Mohammed W. "Analysis of the thermal hydraulics of a multiphase oxygen production reactor in the Cu-Cl cycle." Diss. University of Ontario Institute of Technology (Canada), 2016.
- [4] Abdulrahman, Mohammed Wassef. "Direct contact heat transfer in the thermolysis reactor of hydrogen production Cu—Cl cycle." U.S. Patent No. 10,059,586. 28 Aug. 2018.
- [5] Abdulrahman, Mohammed W. "Scale-up Analysis of Three-Phase Oxygen Reactor in the Cu-Cl Thermochemical Cycle of Hydrogen Production." *Proceedings of EIC Climate Change Technology Conference (CCTC2013)*. 2013.
- [6] Abdulrahman, M. W., Wang, Z., Naterer, G. F., & Agelin-Chaab, M. "Thermohydraulics of a thermolysis reactor and heat exchangers in the Cu-Cl cycle of nuclear hydrogen production." in *Proceedings of the 5th World Hydrogen Technologies Convention*, 2013.
- [7] Abdulrahman, Mohammed W. "Similitude for Thermal Scale-up of a Multiphase Thermolysis Reactor in the Cu-Cl Cycle of a Hydrogen Production." *International Journal of Energy and Power Engineering*, vol. 10, no. 5, pp. 664-670, 2016.
- [8] Abdulrahman, Mohammed W. "Heat Transfer Analysis of a Multiphase Oxygen Reactor Heated by a Helical Tube in the Cu-Cl Cycle of a Hydrogen Production." *International Journal of Mechanical and Mechatronics Engineering*, vol. 10, no. 6, pp. 1122-1127, 2016.
- [9] Abdulrahman, Mohammed W. "Heat transfer in a tubular reforming catalyst bed: Analytical modelling." *proceedings of the 6th International Conference of Fluid Flow, Heat and Mass Transfer*. 2019.
- [10] Abdulrahman, Mohammed W. "Exact Analytical Solution for Two-Dimensional Heat Transfer Equation Through a Packed Bed Reactor." *Proceedings of the 7th World Congress on Mechanical, Chemical, and Material Engineering (MCM'20)*. 2020.
- [11] Abdulrahman, Mohammed W. "Heat Transfer Analysis of the Spiral Baffled Jacketed Multiphase Oxygen Reactor in the Hydrogen Production Cu-Cl Cycle." In *Proceedings of the 9th International Conference on Fluid Flow, Heat and Mass Transfer (FFHMT'22)*, 2022.
- [12] Abdulrahman, Mohammed W. "Thermal Efficiency in Hydrogen Production: Analyzing Spiral Baffled Jacketed Reactors in the Cu-Cl Cycle." *Journal of Engineering Research*, vol. 4, no. 10, 2024.
- [13] Abdulrahman, Mohammed W. "Simulation of Materials Used in the Multiphase Oxygen Reactor of Hydrogen Production Cu-Cl Cycle." *Proceedings of the 6th International Conference of Fluid Flow, Heat and Mass Transfer (FFHMT'19)*. 2019.
- [14] Abdulrahman, Mohammed Wassef. "Material substitution of cuprous chloride molten salt and oxygen gas in the thermolysis reactor of hydrogen production Cu—Cl cycle." U.S. Patent No. 10,526,201. 7 Jan. 2020.
- [15] Abdulrahman, M. W. "Experimental studies of direct contact heat transfer in a slurry bubble column at high gas temperature of a helium–water–alumina system." *Applied Thermal Engineering*, vol. 91, pp. 515-524, 2015.
- [16] Abdulrahman, M. W. "Experimental studies of gas holdup in a slurry bubble column at high gas temperature of a helium– water– alumina system." *Chemical Engineering Research and Design*, vol. 109, pp. 486-494, 2016.
- [17] Abdulrahman, M. W. "Experimental studies of the transition velocity in a slurry bubble column at high gas temperature of a helium–water–alumina system." *Experimental Thermal and Fluid Science*, vol. 74, pp. 404-410, 2016.
- [18] Abdulrahman, Mohammed W., and Nibras Nassar. "Eulerian Approach to CFD Analysis of a Bubble Column Reactor–A." In *Proceedings of the 8th World Congress on Mechanical, Chemical, and Material Engineering (MCM'22)*, 2022.
- [19] Matiazzo, T., Decker, R.K., Bastos, J.C.S.C., Silva, M.K. and Meier, H. "Investigation of Breakup and Coalescence

- Models for Churn-Turbulent Gas-Liquid Bubble Columns." *Journal of Applied Fluid Mechanics* vol. 13, no. 2, pp. 737-751, 2020.
- [20] Schiller, L. (1933). A drag coefficient correlation. *Zeit. Ver. Deutsch. Ing.*, vol. 77, pp.318-320, 1933.
- [21] Ertekin, E., Kavanagh, J.M., Fletcher, D.F. and McClure, D.D. "Validation studies to assist in the development of scale and system independent CFD models for industrial bubble columns." *Chemical Engineering Research and Design*, vol. 171, pp. 1-12, 2021.
- [22] Fletcher, David F., McClure, D.D, Kavanagh, J.M., Barton, G.W. "CFD Simulation of Industrial Bubble Columns: Numerical Challenges and Model Validation Successes." *Applied Mathematical Modelling*, vol. 44, pp. 25–42, 2017.
- [23] Yan, P., Jin, H., He, G., Guo, X., Ma, L., Yang, S. and Zhang, R. "CFD simulation of hydrodynamics in a high-pressure bubble column using three optimized drag models of bubble swarm." *Chemical Engineering Science*, vol. 199, pp. 137-155, 2019.
- [24] Adam, Salman, and Kalthoum Tuwaechi. "Hydraulic Simulation of Bubble Flow in Bubble Column Reactor." *Journal of Complex Flow* vol.1, no.2, Dec. 2019.
- [25] Pourtousi, M., P. Ganesan, and J. N. Sahu. "Effect of bubble diameter size on prediction of flow pattern in Euler–Euler simulation of homogeneous bubble column regime." *Measurement*, vol. 76, pp. 255-270, 2015.
- [26] Abdulrahman, M.W. "CFD Simulations of Direct Contact Volumetric Heat Transfer Coefficient in a Slurry Bubble Column at a High Gas Temperature of a Helium–Water–Alumina System." *Applied Thermal Engineering*, vol. 99, pp. 224–234, 2016.
- [27] Abdulrahman, Mohammed W. "CFD Analysis of Temperature Distributions in a Slurry Bubble Column with Direct Contact Heat Transfer." In *Proceedings of the 3rd International Conference on Fluid Flow, Heat and Mass Transfer (FFHMT'16)*. 2016.
- [28] Abdulrahman, Mohammed W. "CFD Simulations of Gas Holdup in a Bubble Column at High Gas Temperature of a Helium-Water System." In *Proceedings of the 7th World Congress on Mechanical, Chemical, and Material Engineering (MCM'20)*, 2020.
- [29] Abdulrahman, Mohammed W. "Effect of Solid Particles on Gas Holdup in a Slurry Bubble Column." In *Proceedings of the 6th World Congress on Mechanical, Chemical, and Material Engineering*, 2020.
- [30] Abdulrahman, Mohammed W. "Temperature profiles of a direct contact heat transfer in a slurry bubble column." *Chemical Engineering Research and Design*, vol. 182, pp. 183-193, 2022.
- [31] Abdulrahman, Mohammed W., and N. Nassar. " Three Dimensional CFD Analyses for the Effect of Solid Concentration on Gas Holdup in a Slurry Bubble Column." *Proceedings of the 9th World Congress on Mechanical, Chemical, and Material Engineering (MCM'23)*. 2023.
- [32] Abdulrahman, Mohammed W., and N. Nassar. " A Three-Dimensional CFD Analyses for the Gas Holdup in a Bubble Column Reactor." *Proceedings of the 9th World Congress on Mechanical, Chemical, and Material Engineering (MCM'23)*. 2023.
- [33] Abdulrahman, Mohammed W., and N. Nassar. " Effect of Static Liquid Height on Gas Holdup of a Bubble Column Reactor." *Proceedings of the 9th World Congress on Mechanical, Chemical, and Material Engineering (MCM'23)*. 2023.
- [34] ANSYS Inc. "ANSYS FLUENT Theory Guide." ANSYS FLUENT Theory Guide, Version 14.5, 2012.